

U.S. DEPARTMENT OF THE INTERIOR

U.S. GEOLOGICAL SURVEY

Late Cretaceous shortening  
and Cenozoic extension  
in the northern Madison Range,  
southwestern Montana

by

Karl S. Kellogg<sup>1</sup>

Open-File Report 94-147

This report is preliminary and has not been reviewed for  
conformity with U.S. Geological Survey editorial standards.

<sup>1</sup> U.S. Geological Survey  
Box 25046, MS 913  
Denver Federal Center  
Denver, CO 80225

Late Cretaceous thrusting and Cenozoic extension  
in southwestern Montana--view from the northern Madison Range

---

Karl S. Kellogg U.S. Geological Survey, Box 25046, MS 913,  
Denver Federal Center, Denver, Colorado 80225

ABSTRACT

Two major Laramide fault systems converge in the northern Madison Range: (1) the northwest-trending Spanish Peaks fault, a high-angle reverse fault that places Archean rocks on the north-east against rocks as young as Early Cretaceous on the southwest, and (2) the north-trending Hilgard thrust system, the eastern edge of the east-directed Madison-Gravelly basement arch. The hanging wall of the Spanish Peaks fault buttressed movement on the Hilgard thrust system, so substantial movement on the Spanish Peaks fault predates movement on the Hilgard system. Analysis of foliation attitudes north and south of the Spanish Peaks fault indicates that the basement in thrust blocks of the Hilgard thrust system has rotated by an amount similar to that of the basement-cover contact. North-striking breccia zones within the rotated blocks enclose domains of relatively undeformed basement, suggesting a model for basement thrusting and rotation involving numerous imbricate backthrusts.

In most places along the Hilgard thrust system, a large basement overhang, produced by thrusting of Archean blocks above rocks as young as Late Cretaceous, overlies a tight footwall syncline. This tight folding was accommodated by flexural slip, resulting in such secondary features as hinge collapse (as at Jack Creek) and cross-crestral thrusting (as at Shell Creek).

The north-trending Madison fault system, a zone of Tertiary and Quaternary valley-forming normal faults, is approximately parallel to the Hilgard thrust system. Movement along the Madison fault system may have begun as long ago as the middle Eocene, when crustal extension commenced. In some places, the large basement overhangs of the Hilgard thrust system are entirely dropped back into the Madison Valley, leaving only the rocks of the footwall synclines exposed. In other places, both the thrust blocks and the near-isoclinal footwall synclines are well preserved. Younger-over-older normal faults commonly are reactivated along former thrusts.

The Hilgard thrust system is similar to other Laramide thrust systems in southwestern Montana that also define the eastern margins of large basement arches. In each case, collapse of the crestral zones of the arches during Tertiary crustal extension formed systems of paired valley-forming normal faults and range-bounding thrust faults; the paired fault systems bound elevated wedges of basement rock (perched basement wedges). The paired fault system in the northern Madison Range, the Madison normal fault system and the Hilgard thrust system, is strikingly similar to other paired systems in southwestern Montana along and adjacent to the western margins of the Ruby Range, Snowcrest Range, Tobacco Root Mountains, and Bridger Range.

## INTRODUCTION

The Madison Range, extending north from the northwestern corner of Yellowstone National Park, lies within the Laramide foreland province of southwestern Montana. The west side of the range contains the Hilgard thrust system (Tysdal, 1986), produced by generally east-west contraction and thrusting of Archean basement blocks over sedimentary rocks as young as Late Cretaceous (Fig. 1). In the northwestern part of the range, large topographic relief and steep canyon walls create excellent exposures of this thrust system and the tight hinge zones of the underlying footwall synclines. This part of the Laramide foreland province also lies at the northeastern margin of the Basin and Range province defined by the intermountain seismic belt (Smith and Sbar, 1974). The Madison Valley, a deep, north-trending Tertiary half graben typical of the Basin and Range province, bounds the Madison Range on the west.

### Figure 1 near here

The northwest-trending Spanish Peaks fault, recognized in the last century (Peale, 1896), is a major structural feature of southwestern Montana that was first mapped in detail by Swanson (1950). Garihan and others (1983) described the Spanish Peaks fault and its northwestern and southeastern extensions. On the northwest side of the Madison Range, the Spanish Peaks fault intersects the generally north-striking Hilgard thrust system, the northern part of which was mapped by Swanson (1950) and Young (1985). Tysdal and Simons (1985) mapped the Hilgard thrust system farther to the south. The zone of interaction between the Spanish Peaks fault and the Hilgard thrust system has been investigated by Swanson (1950), Tonnsen (1982), Garihan and others (1983), and Young (1985). Tysdal (1986) incorporated Swanson's work into an overall tectonic model for Laramide deformation in the Madison Range, one in which many east-dipping structures along the Hilgard thrust system were explained as back thrusts. Tysdal and others (1986) observed that a dacite porphyry sill complex, dated by the  $^{40}\text{Ar}/^{39}\text{Ar}$  method at about 68-69 Ma, intruded Laramide-age thrusts, indicating a minimum age for deformation.

The purpose of this paper is to examine various structural processes that shaped the northern Madison Range, such as the mechanism by which tight footwall synclines formed beneath thrustured basement blocks (basement overhangs), the timing of Laramide contraction and Tertiary extension, and the extent to which Tertiary deformation was controlled by earlier Laramide structures. I also present a model for the apparent rotation of basement-cored thrust blocks that is consistent with the observed structures. I point out, as others have noted (Schmidt and others, 1984; Lageson and Zim, 1985; McBride and others, 1992), that the processes that formed the northern Madison Range are typical of a style of deformation that influenced a large part of southwestern Montana.

## GEOLOGIC SETTING

The western flanks of many southwestern Montana mountain ranges expose thrust faults that have placed basement crystalline rocks over rocks as young as Late Cretaceous (Fig. 1). These ranges include the Snowcrest Range (Sheedlo, 1984), the Greenhorn Range (Berg, 1979; Hadley, 1969), the Ruby Range (thrust structure inferred by Schmidt and Garihan, 1986, from mapping by Tysdal, 1976; R.G. Tysdal, oral commun., 1991), the Tobacco Root Mountains (O'Neill, 1983; Samuelson and Schmidt 1981), and the Madison Range (Tysdal, 1986; Kellogg, 1992, 1993a). A blind thrust underlies the Bridger Range (Lageson, 1989), but otherwise its structure is similar to that of these other southwestern Montana ranges.

Along the western side of the Madison Range, well-exposed thrust faults and associated folds on the Hilgard thrust system can be traced southeastwardly into the interior part of the range. In the central part of the range, the youngest unit involved with thrusting is the synorogenic Sphinx Conglomerate (DeCelles and others, 1987), which crops out a few kilometers south of the study area (symbol TKi in Figure 1). The Hilgard thrust system defines the eastern margin of a large north- to northwest-trending basement high originally named the Madison-Gravelly arch by Scholten (1967).

The Spanish Peaks fault, including its northwestern and southeastern extensions, is the most continuous member of a set of parallel, northwest-striking reverse faults that cross southwestern Montana (Schmidt and Garihan, 1983; Garihan and others, 1983) (Fig. 1). Young (1985) inferred that Laramide movement on the Spanish Peaks fault was left-lateral oblique, similar to that observed for virtually all the northwest-trending high-angle reverse faults of southwestern Montana (Schmidt and Garihan, 1986). These faults are thought to have been active since the Middle Proterozoic (Reid, 1957; Schmidt and Garihan, 1986), based in part on the occurrence of Middle Proterozoic dikes (Wooden and others, 1978) that trend approximately parallel to, and locally intruded, the faults.

Starting in middle Eocene time, broad Tertiary extensional basins, largely filled by lacustrine sedimentary rocks, began to form across southwestern Montana (Pardee, 1950; Kuenzi and Fields, 1971; Hanneman and Wideman, 1991). The present narrow extensional valleys began forming in the middle Miocene during more rapid extension and were filled with clastic, commonly conglomeratic sediments (Fields and others, 1985). During Neogene valley formation, structural inversion occurred along the crestral zone of many of the foreland thrusts (Schmidt and others, 1984). Dondropping of the northeastern side of the Madison Valley was accomplished in part by backsliding along older faults of the Hilgard thrust system (Werkema and Young, 1983; Young, 1985). Farther south, where the Hilgard thrust system curves eastward into the Madison Range, subsidence occurred along listric normal faults that are high-angle at the surface and probably sole into older thrusts. The Madison Valley is a deep extensional half graben faulted down along the eastern side and filled south of Ennis with about as much as 4,500 m of Tertiary

and Quaternary sediments (Rasmussen and Fields, 1983). Along the east side of the Madison Valley, the Quaternary Madison Range fault system of Pardee (1950) is still active; parts of the fault system were reactivated during the 1958 Hebgen Lake earthquake (U.S. Geological Survey, 1964). A number of spectacular late Quaternary fault scarps are present at the base of the mountain front.

The Spanish Peaks fault appears inactive since at least Eocene time, because unfaulted volcanic rocks of the Eocene Absaroka volcanic field overlap the southeast end of the fault (Garihan and others, 1983). The northwest extension of the Spanish Peaks fault coincides with the position of the North Meadow Creek normal fault (Fig. 1), which defines the northern structural margin of the Madison Valley, suggesting that the locus of Tertiary normal displacement was governed by the position of the faulted edge of the uplifted Archean block. Kellogg (1983b) inferred that displacement on the North Meadow Creek fault was coeval with opening of the Madison Valley, implying that fault movement is as old as middle Miocene. Young (1985) reported that about 40 m of post-Miocene(?) down-to-the-southwest displacement occurred along the North Meadow Creek fault.

Although faults of the Madison Range fault system may sole into Laramide-age thrusts, they are neither parallel to nor exactly coincident with the Hilgard thrust system. In the west-central part of the range, most of the Hilgard thrust system has been entirely downdropped into the Madison Valley. To the south, the Hilgard thrust system trends obliquely into the range, away from the valley margin and its associated normal faults.

## STRATIGRAPHY

The stratigraphic sequence exposed above Archean crystalline rocks in the northern Madison Range is typical of the stable cratonic shelf of southwestern Montana and consists of mostly carbonate-rich rocks of Middle Cambrian to Mississippian age overlain by mainly clastic deposits of late Paleozoic and Mesozoic age. The exposed sequence within the study area (Fig. 2) is about 3,000 m thick, about half of which is Cretaceous in age.

---

### Figure 2 near here

For the purposes of this paper, the Phanerozoic rock units are grouped into nine map units above the Archean crystalline basement. Detailed stratigraphic descriptions are given in Tysdal and Simons (1985) and Kellogg (1992). The basement rocks consist mostly of high-grade quartzofeldspathic gneiss and amphibolite with subordinate amounts of dolomitic marble, aluminous schist and gneiss, quartzite, and pods of ultramafic rocks.

## LARAMIDE (LATE CRETACEOUS TO EARLY EOCENE) DEFORMATION

### Spanish Peaks Fault

The Spanish Peaks fault was discussed in detail by Garihan and others (1983). Within the map area of Figure 2, the fault strikes about N. 60° W. Imbricate fault slices between steeply dipping panels of Phanerozoic rocks appear discontinuously south of the fault. The dip of the Spanish Peaks fault ranges from about 70° NE to vertical (Garihan and others, 1983). The fault itself is rarely exposed but can be located in most places within about 20-30 m, which limits the precision to which the attitude of the fault can be determined from the topographic expression. Minimum throw on the Spanish Peaks fault is about 4,100 m, based on structural relief between the highest Archean outcrops north of the fault and the buried base of the Cambrian south of the fault (McMannis and Chadwick, 1964).

Attitudes of a limited number of striations from slickensided surfaces along small splays parallel to the Spanish Peaks fault suggest approximately equal amounts of left-lateral strike-slip and reverse dip-slip faulting (Garihan and others, 1983; Young, 1985). A large number of striations measured from other northwest-striking, up-to-the-northeast basement faults in southwestern Montana also indicate about equal amounts of dip-slip and left-lateral strike-slip displacement, which is consistent with an approximate east-west direction of greatest principal stress during the Laramide orogeny (Schmidt and Garihan, 1983, 1986). Erslev (in press) presents evidence, however, that the Laramide orogeny in the northern Rocky Mountains was characterized overall by northeast-southwest compression.

### The Hilgard Thrust System

The Hilgard thrust system (Tysdal, 1986) comprises a number of imbricate thrust faults that strike roughly parallel to the Madison Range mountain front (Fig. 2). The discussion which follows examines the Hilgard thrust system from its northernmost extent, where thrust geometry and net displacement is clearly influenced by the Spanish Peaks fault, to a point about 16 km to the south. Five cross sections (Figs. 3A-3E) across the thrust system will be examined.

Figure 3 near here

**Zone of Impingement Between the Hilgard Thrust System and the Spanish Peaks Fault System (Fig. 4).** Net thrust separation decreases northward from approximately Jack Creek toward the impingement zone between the Hilgard thrust system and the Spanish Peaks fault (Fig. 5), indicating that a pre-existing Spanish Peaks fault acted as a buttress against movement by the Hilgard thrust system, an interpretation also made by Young (1985). The trace of the fault does not appear to have been significantly refracted in the region of intersection with the Hilgard thrust system. This does not, however, eliminate the

possibility of some coeval movement along the Spanish Peaks fault and the Hilgard thrust system, or movement along the Spanish Peaks fault after movement along the Hilgard thrust system had ceased.

Figures 4 and 5 near here

Total dip-slip thrust separation near Jack Creek is about 5,500 m. Previous mapping showed the fault displacement decreasing to zero about 3.0 km north of Jack Creek, with east-directed contraction north of this point accommodated by folding (Swanson, 1950; Garihan and others, 1983; Young, 1985). However, detailed mapping of Cretaceous units above the Kootenai Formation demonstrates that previously unrecognized faults of the Hilgard thrust system have significant offsets within a few hundred meters of the Spanish Peaks fault (Kellogg, 1993b). Unfortunately, the region of intersection is hidden under Quaternary cover, so it is not possible to determine the nature of the actual zone of interaction. At their northernmost exposures, about 300 m south of the intersection, faults of the Hilgard thrust system show a combined offset of several hundreds of meters.

Cross sections A-A' (Fig. 3A) and B-B' (Fig. 3B) show several additional features characteristic of the impingement zone between the Spanish Peaks fault and the Hilgard thrust system: (1) the dip of the thrusts increases to the north along the Hilgard thrust system, (2) the amount of overturning in the Paleozoic rocks decreases to the north, and (3) the two northernmost splays of the Hilgard thrust system curve to the west (Fig. 2) and are spoon shaped in three dimensions.

**Exposed Structures Adjacent to Jack Creek.** North of Jack Creek, the westernmost thrust of the Hilgard thrust system (location 1 on Figure 2; herein called the Jack Creek thrust after Young, 1985) ramps northward to structurally higher levels. At most places, the Jack Creek thrust places Archean rocks above overturned Paleozoic or Mesozoic rocks. Adjacent to Jack Creek, Archean rocks in the hanging wall of the Jack Creek thrust overlie overturned Mississippian Lodgepole Limestone. East of the Jack Creek thrust, gently dipping overturned units are well exposed in an imbricate fan (Fig. 3C). Map patterns indicate that all of the thrust faults dip about 35° to the west.

Structures near Jack Creek reveal several interesting features:

1. The fold produced by thrusting of the large Archean basement block apparently underwent hinge collapse (Ramsay and Huber, 1987, p. 424); the less-competent Upper Cretaceous rocks apparently moved out of the fold hinge zone by flexural slip or flow (cf., Donath and Parker, 1964), accompanied by progressive collapse of older, more competent units on the two limbs of the fold toward each other (i.e., toward the hinge zone). Hinge collapse does not necessarily imply that units in the hinge zone are either thinned or discordantly deformed. In fact, Cretaceous rocks within the hinge zone, both overturned and upright, do not appear to be significantly deformed.

2. Folding was accommodated by bedding-parallel slip, as indicated by two observations. Overturned, commonly nearly

horizontal rocks of the Mowry Shale and Muddy Sandstone are virtually undeformed in outcrop, suggesting that flexural flow may have been of minimal importance. In addition, the overturned Kootenai Formation and Mowry Shale, the only Cretaceous units in the overturned limb for which thickness could be determined, do not appear to be abnormally thin. This suggests that passive flow, the movement of material across unit boundaries, did not accompany folding.

3. Cross-section C-C' shows structures that are remarkably similar to those beneath buried basement overhangs, such as described by Berg (1962) in unrestorable cross sections derived from seismic and well data along the Wind River thrust in Wyoming.

**Structures Between Jack Creek and Cedar Creek.** About 1 km south of Jack Creek, the Jack Creek thrust ramps to the south in the footwall laterally upsection to the Permian Shedhorn Sandstone (location 2 in Fig. 2). At this point, the thrust converges with a fault interpreted to be a Tertiary normal fault, south of which the thrust once again juxtaposes Archean rocks above the Lodgepole Limestone. At location 3 in Figure 2, several small Archean-cored thrust-bounded blocks, in which the Flathead Sandstone crops out with apparent depositional contact with basement rocks, overlaps the frontal thrust. The small blocks show a complex geometry and contain a variety of bedding and foliation orientations. This geometry probably formed during Tertiary extension, manifested largely by backsliding along former thrust faults. South of location 3, the Jack Creek thrust is covered by Quaternary and Tertiary basin-fill deposits and is inferred to have been dropped down into the Madison Valley along Tertiary normal faults. The probable southward extension of the Jack Creek thrust reappears in the southernmost part of the study area (location 4 in Fig. 2).

South of location 3, a tight asymmetrical syncline with nearly planar limbs characterizes the deformation (Fig. 3D). The western limb of the syncline is steep to overturned whereas the eastern limb dips gently to the west. In most places, the steep western limb and axial-plane region are cut by numerous thrust faults that have placed older rocks over younger rocks.

**Structure between Cedar Creek and 2 km south of Shell Creek.** Most of the range front between Cedar Creek and Shell Creek is dominated by nearly vertical, prominently outcropping beds of Madison Group limestone, which form the overturned western limb of a large east-vergent recumbent syncline (Figs. 3E and 6). Basement is inferred to have been thrust above the western limb of the syncline but has since slid back into the Madison Valley along range-bounding normal faults. The easternmost normal fault probably occupies about the same position as the inferred basement thrust (the southern extension of the Jack Creek thrust) that produced the recumbent syncline.

#### Figure 6 near here

The eastern limb of the syncline is nearly flat lying. All rocks exposed in Shell Creek are stratigraphically above the Madison Group and include a thick sequence of Mississippian and Pennsylvanian Snowcrest Range Group rocks.

On the steep northern side of Shell Creek canyon, just north of cross-section E-E', the Jurassic and Triassic section is over twice its normal stratigraphic thickness of about 500 m. Small-scale thrust imbrication in and near the hinge zone of the tight syncline, although not observed in the field, are believed to have caused the thickening, as indicated on cross-section E-E', in which structures on the north wall of the canyon are projected onto the plane of the cross section. The imbricate splay merges eastward into a single bedding-parallel thrust fault named the Shell Creek thrust (described as a cross-crestal thrust by Kellogg, 1990), which steepens eastward and is spectacularly exposed on the north canyon wall. East of the short bedding-parallel section, the thrust ramps upsection toward the east in both the hanging wall and footwall, which strongly suggests that the thrust is not a west-directed back thrust but, instead, an out-of-syncline thrust. Stratigraphically above the Kootenai Formation in the footwall, the thrust is not exposed but I infer it ramps upsection into Cretaceous shales and sandstones--about the middle of the Mowry Shale--where it probably flattens and dies out.

A conspicuous result of the thrusting in Shell Creek is the repetition of the basal Kootenai Formation sandstone. In the footwall, it forms a prominent, vertically dipping outcrop across the bottom of the creek; directly above, in the hanging wall, the Kootenai is nearly horizontal. Several hundred meters to the east, the Kootenai progressively dips more eastward.

Rocks in the footwall of the Shell Creek thrust, specifically the Pennsylvanian Quadrant and Permian Shedhorn Sandstones, are folded into a tight, east-vergent chevron anticline. This structure had previously been interpreted as a thrust window (Swanson, 1950) bounded on the east by the Shell Creek thrust and on the west by a continuation of the Shell Creek thrust along the axial surface of the chevron anticline. Except for small-scale bedding slip in the hinge zone of the chevron anticline, however, there does not appear to be any significant offset along the axial surface.

Restoration of the structures in Shell Creek to their inferred pre-extensional geometry reveals a great deal about the kinematics of deformation. Figure 7 is an area-balanced, pre-Tertiary-extension cross section. The restoration demonstrates that a maximum of about 0.5 km of dip-slip displacement occurred along the Shell Creek thrust. It also serves to point out that without the presence of the chevron anticline, probably a fault-propagation fold above a hidden basement thrust, movement along the Shell Creek thrust might have been confined entirely to bedding planes within the Jurassic or Triassic rocks. Without the presence of the chevron fold, the effects of accommodation to tight folding in the footwall syncline might have been overlooked.

---

Figure 7 near here

South of Shell Creek, two normal faults downdrop the gently dipping Kootenai Formation in a step-like manner. At the southern margin of the study area, a block of white, coarse-grained, Archean dolomitic marble is thrust above a thrust-bounded sliver

of Middle Jurassic Rierdon Limestone that is in turn thrust above several thrust-bounded blocks or wedges of Cretaceous rock.

### Basement Involvement in Laramide Deformation

An active debate concerns the character and role of basement deformation in Laramide uplifts (e.g. Chase and others, in press). The development of metamorphic foliation and the relationship of basement foliation attitudes to bedding attitudes in the overlying folded rocks seems to be a critical factor governing whether basement rocks folded by flexural slip (Schmidt and Chase, 1989; Schmidt and others, in press; Miller and Lageson, in press). Where rocks are relatively isotropic and foliation is highly oblique to bedding in the overlying sedimentary rocks, little or no basement folding apparently occurred and deformation was largely fault controlled. Where relatively well-developed basement foliation is nearly parallel to the basement-cover contact, folding was by flexural slip. Erslev and Rodgers (in press) have a somewhat different view; they show that Laramide uplifts can be modeled as an assemblage of rigid blocks and that only limited basement bending occurs near the overhanging tips of the uplifts.

Preliminary investigations north of Jack Creek and south of the Spanish Peaks fault by Werkema and Young (1983) suggested that basement was folded about axes parallel to fold axes in the overlying Phanerozoic rocks. Further detailed work by Young (1985), however, did not support this hypothesis; no evidence for basement folding could be demonstrated in the fault blocks west of the Hilgard thrust system. Likewise, little evidence was found for Laramide basement folding north of the Spanish Peaks fault (Garihan and others, 1983).

Foliation adjacent to both the Spanish Peaks fault and the Hilgard thrust fault system is nearly perpendicular to both the attitude of the faults and the overlying Phanerozoic strata (Fig. 2; Kellogg, 1992, 1993a), which helps to explain why no basement folding was found by Young (1985) in the study area. In addition, the basement-cover contact north of Jack Creek probably is unfaulted (Werkema and Young, 1983), although I did not observe an unequivocal depositional contact. However, the Cambrian Flathead Sandstone, the basal unit, appears to crop out continuously for about 4 km and no zones of brecciation within basement rocks were observed within or immediately adjacent to the Flathead. At several other localities in southwestern Montana, steeply dipping unfaulted basement-cover contacts were observed (Schmidt and Chase, 1989).

It seems reasonable that basement unconformably underlying steeply dipping cover rocks is likewise rotated, yet it is not proven. Models using distributed basement shear along closely spaced fractures (e.g. Spang and others, 1985) explain the apparent rotation and folding of the basement-cover contact, but do not necessarily conserve angular relationships between basement structures (such as foliation) and the contact. Spang and Evans (1988) suggest that distributed shear may explain the rotations in the northern Madison Range.

The following analysis tests whether foliation attitudes

within gneissic basement north and south of the Spanish Peaks fault are consistent with rigid-body rotation by an amount equal to the dip of the basement-cover contact. If one assumes that the block north of the Spanish Peaks fault was not significantly rotated during Laramide deformation, as is suggested by the near-vertical attitude of the Spanish Peaks fault and the size of the block to the north (it extends approximately 18 km to the northeast of the Spanish Peaks fault; Fig. 1), then the mean foliation attitude within a small domain immediately north of the fault (location 5A within the dashed line shown in Fig. 2) can be used as a reference with which to compare rotation south of the fault (Fig. 8). The data, although somewhat scattered, defines a maximum pole to foliation at  $D$  (declination) =  $130^{\circ}$ ,  $I$  (inclination) =  $30^{\circ}$ . Within the block directly south of the Spanish Peaks fault (location 5B in Fig. 2), a well-defined maximum pole to foliation is  $D = 185^{\circ}$ ,  $I = 42^{\circ}$ . The difference in foliation attitude between the two maxima is about  $60^{\circ}$ , in a sense compatible with down-to-the-east rotation of the block south of the Spanish Peaks fault. The mean attitude from 7 observations of Cambrian beds within block 5B is  $57^{\circ}$ , in good agreement with a model in which basement was rotated by the same amount as the basement-cover contact.

Figure 8 near here

Rigid-body rotations of more than several tens of degrees of large, undeformed basement blocks are unrestorable (Erslev, 1986; in press); clearly, some mechanism either of distributed or commutated shear must be invoked to accommodate the rotation. Within basement gneiss exposed near Jack Creek west of the Jack Creek thrust, north-striking breccia zones as wide as about 10 m have been locally mapped (Young, 1985; Kellogg, 1992, in press; Fig. 2). Additional unmapped breccia zones undoubtedly exist and many are hidden under surficial deposits. To further complicate matters, some breccia zones near Jack Creek probably are related to Tertiary extension, as strongly suggested by the dense concentration of breccia zones adjacent to the basin-fill deposits of the Madison Valley.

Significant cataclasis within thrust basement blocks that contain steeply dipping to overturned basement-cover contacts occurs elsewhere in southwestern Montana. For example, about 9 km south of the study area, extensive zones of cataclasis cut basement rocks above the locally low-angle Scarface thrust (Schmidt and others, in press). In addition, about 15 km south of Bozeman in the northern Gallatin Range (Fig. 1), where foliation attitudes are at a high angle to the basement-cover contact, blocks of undeformed basement gneiss were displaced relative to one another along numerous zones of cataclasis (Miller and Lageson, in press).

A model for basement rotation, consistent with the geologic observations, is schematically outlined in Figure 9. During thrusting, irregularly shaped, fault-bounded panels of basement rock within a basement wedge remain approximately parallel to the basement-cover contact. The panels rotate and slide domino style along imbricate back thrusts that commonly develop as zones of cataclasis. The "space problem" that develops at the ends of the

panels, adjacent to the major wedge-bounding thrust faults, is accommodated by pervasive cataclasis and rotation of small breccia-bounded blocks. Note that with a basement rotation of more than  $90^{\circ}$  (as is the case in the basement block traversed by Jack Creek), the panel-bounding faults become apparent normal faults; such faults may become easily reactivated during Tertiary extension. Note also that if this model is valid, it requires that a major basement-involved thrust lay to the west of the Jack Creek thrust but was apparently downdropped during Tertiary extension into the Madison Valley.

#### **LATE CRETACEOUS MAGMATISM**

The laccolith complex under Fan Mountain (Fig. 3D) domed the sedimentary sequence and created approximately 750 m of structural relief. Swanson (1950) called the intrusive structure underlying Fan Mountain a "Christmas-tree laccolith," although Kellogg (1992) presents evidence that there is no central feeder pipe ("tree trunk"); instead, most feeder dikes cut obliquely upsection from one sill to another, as shown in Figure 3D. Kellogg (1992) informally called the intrusive rock the dacite porphyry of Fan Mountain.

Tysdal and others (1986) reported slightly discordant K/Ar (potassium/argon) and  $^{40}\text{Ar}/^{39}\text{Ar}$  hornblende dates of about 68-69 Ma from localities in the dacite porphyry south of the study area. These dates are supported by a slightly discordant  $^{40}\text{Ar}/^{39}\text{Ar}$  date of  $68.7 \pm 0.3$  Ma on hornblende from a site in Jack Creek (S.S. Harlan, written commun., 1991) (location 6 in Fig. 2). Thus, 68-69 Ma best represents the age of the dacite porphyry, although this is not in agreement with a K/Ar biotite date of  $57.7 \pm 1.4$  Ma for a probably correlative porphyritic dike (DeCelles and others, 1987) that intrudes the synorogenic Sphinx Conglomerate about 10 km south of the map area.

Accurate dating of the dacite porphyry of Fan Mountain is crucial for constraining the timing of Laramide deformation. Dacite porphyry intruded fault surfaces of the Hilgard thrust system (Tysdal and others, 1986), interpreted to indicate that Laramide deformation predates 68-69 Ma. Preliminary paleomagnetic evidence also indicates that most if not all Laramide deformation predates emplacement of the sills (Kellogg and Harlan, 1991). Laramide deformation must also be younger than about 76 Ma, the approximate K/Ar date for biotite from a tuff in the lower part of the Livingston Group (Tysdal and others, 1986), which directly underlies the Sphinx Conglomerate.

#### **QUATERNARY AND TERTIARY EXTENSION**

The geometry of Laramide thrusting and folding was complicated by Tertiary normal faulting. Pardee (1950 and Swanson (1950) both recognized large-scale Tertiary normal faults, as well as Quaternary fault scarps cutting basin-fill deposits, along the Madison Range front. Many of the normal faults mapped in the northern Madison Range merge laterally with thrusts (e.g., location 2 in Fig. 2), supporting the suggestion of Werkema and Young (1983), discussed further by Young (1985),

that normal faults flatten and merge at depth with thrusts and that backsliding was accommodated along the former thrust surface.

Large internally brecciated fault blocks composed mostly of Madison Group limestone, but also including Pennsylvanian Quadrant Sandstone and Jurassic Morrison Formation, are exposed near the western end of Figure 3D and represent large gravity slides into the Madison Valley. Presently, none of the rocks represented in these slide blocks is exposed in bedrock outcrops directly upslope to the east, which indicates that sliding occurred at a time when the topography was substantially different from what it is today, probably during the Pliocene or Miocene.

Tertiary normal faulting associated with the formation of the Madison Valley accounts for the downdropping and burial of large segments of the Jack Creek thrust that, prior to middle Eocene time, probably extended continuously south of the Spanish Peaks fault. Thus, the style of deformation exposed along the front of the Madison Range largely reflects the position of the Jack Creek thrust with respect to the major normal faults that define the range front. South of a point about halfway between Jack and Cedar Creeks to near Shell Creek, the Jack Creek thrust has been entirely downdropped into the Madison Valley; only portions of the footwall syncline that formed beneath the frontal thrust remain exposed. Southward from the southern boundary of the study area (Fig. 1), the Hilgard thrust system is exposed progressively more to the east of the range front (Tysdal and Simons, 1985; Tysdal, 1986).

## DISCUSSION

Two types of basement-involved deformation in the northern Madison Range during Late Cretaceous and early Tertiary time, represented by the Spanish Peaks fault and the Hilgard thrust system, were the result of generally east-directed contraction. Failure along the Spanish Peaks fault, similar to that along other northwest-oriented high-angle reverse faults in southwestern Montana, was influenced strongly by pre-existing northwest-striking planes of weakness that were established at least as early as Middle Proterozoic time (Schmidt and Garihan, 1986). However, no preexisting planes of weakness apparently influenced the emplacement of the Hilgard thrust system.

The Hilgard thrust system forms the eastern edge of the large Madison-Gravelly arch (Scholten (1967). Schmidt and others (1984) and Sheedlo (1984) suggested that this basement arch formed as a large ramp anticline above westward-dipping listric thrusts, similar to other basement arches in southwestern Montana. Structures within Phanerozoic rocks are therefore the result of passive deformation associated with active basement thrusting. Figure 10 is a cross section across the Madison Range, northern Greenhorn Range, and the northern Ruby Range that integrates the basement-arch model with information from COCORP deep-seismic profiling across the Wind River Mountains in Wyoming (Sharry and others, 1986). The line of cross section is shown on Figure 1. The Wind River Mountains is a basement uplift that is

geometrically similar to the Madison-Gravelly arch except that the vergence direction of the range-bounding Wind River thrust is to the southwest and is buried. The Wind River thrust is listric and soles into a complex mid-crustal duplex zone at about 15-25 km depth (Sharry and others, 1986).

Figure 10 near here

At the close of the Laramide orogeny (Fig. 10A), thick synorogenic conglomerates (unit TKc), derived from the erosion of the major basement arches, were deposited on the foreland side of the arches. The erosional remnants of the synorogenic conglomerates (Fig. 1) are now represented in southwestern Montana by the Beaverhead Conglomerate and the Sphinx Conglomerate (DeCelles and others, 1987).

Backthrusting within Phanerozoic rocks does not appear to be an important feature of Laramide thrusting in the northern Madison Range, although it appears to play a significant role farther to the south (Tysdal, 1986, 1990). Backthrusts in the basement rocks may also have accommodated basement rotation. At least one fault in the northwestern Madison range, the Shell Creek thrust (Fig. 3E), is east-dipping and might easily be mistaken for a back thrust, although it is interpreted here to be east directed.

The general coincidence of Tertiary basins in southwestern Montana with the axial zones of large basement arches (Fig. 1) is one of the most curious features of the region. Although the coincidence is striking, the distances between the east margins of the basins and the Laramide thrusts vary considerably, and in some places, such as near Twin Bridges in the Beaverhead Valley (Fig. 1) and near Shell Creek in the Madison Valley, the basin margins overlap the thrusts. In other places, such as in the southern part of the Madison Range, the basin margins lie considerably west of the thrusts. Nonetheless, the coincidence of basins with the axial zones of basement arches, and the positions of major thrusts generally along the western mountain fronts, suggest a genetic relationship between the arches and the valleys.

Tertiary basins in southwestern Montana may be a direct consequence of Laramide thrusting (Schmidt and others, 1984; Sheedlo, 1984; Lageson and Zim, 1985; McBride and others, 1992). Extensional fractures or zones of weakness that developed in the crests of ramp anticlines during Laramide thrusting later became sites of Tertiary extensional faulting that ultimately produced north-trending valleys. Sites of such "structural inversion" (Schmidt and Dresser, 1984) include not only the Madison Valley, but the Beaverhead Valley, the Ruby River Valley, and the Gallatin Valley (Fig. 1), all of which formerly occupied the crestral zones of large basement arches.

The formation of paired valley-and-thrust systems leaves an elevated wedge of basement along the range front, bounded on the east by one or more thrust faults and on the west by one or more normal faults. Such features in the Bridger Range (Fig. 1) were called "perched basement wedges" (Lageson and Zim, 1985; Lageson, 1989), although the thrusts which bound the basement wedges are almost completely blind. Good examples of perched basement

wedges are shown in Figures 3A-3D.

The formation of paired valley-and-thrust systems, and the associated formation of perched basement wedges, may be important processes anywhere contraction is followed by opposite-directed extension. Schmidt and Dresser (1984) caution, however, that structural inversion may be obscured where extension is greater than about 10 percent (the interpretation shown in Figure 10B shows about 10 percent east-west Tertiary extension).

A good example of structural inversion in northern New Mexico is exposed along the west side of the generally north-trending Sangre de Cristo Mountains adjacent to the Mora Valley (Baltz and O'Neill, 1984). Basement gneiss has been thrust above sedimentary rocks as old as Mississippian, producing a paired valley-and-thrust system and a perched basement wedge, remarkably similar to those found throughout southwestern Montana. Other examples of paired valley-and-thrust systems and their associated perched basement wedges are noted by Lageson and Zim (1985).

## CONCLUSIONS

The observations are consistent with the following conclusions:

1. Thrusting of basement and cover rocks along the northwestern side of the Madison Range during the Late Cretaceous produced a tight, east-facing footwall syncline in Paleozoic and Mesozoic rocks. In order to accommodate tight folding in the footwall as the basement wedge moved up and eastward, secondary accommodation features developed mostly by bedding-parallel slip and small-scale ramping. Such features include hinge collapse, as at Jack Creek, and out-of-syncline thrusting, as at Shell Creek.

2. Restorable models for Laramide uplift and rotation must also accommodate at least localized rotation of the basement by an amount compatible with the attitude of the basement-cover contact. A model for basement thrusting and rotation along the Hilgard thrust system involving imbricate backthrusts accounts for both rotation of the basement and observed north-striking breccia zones within the thrust block.

2. The formation of the paired Madison (normal) fault system and the Hilgard thrust system was similar to that of other paired normal and thrust systems in regions that have undergone shortening followed by small extensional strain (Schmidt and Dresser, 1984). The Madison Valley probably formed during middle Miocene time along the crestal zone of the Madison-Gravelly arch by exploiting zones of weakness or fractures that formed during Late Cretaceous thrusting (Schmidt and others, 1984). However, the distance between valley margins and the arch-bounding thrusts varies considerably. Late Cenozoic range-front normal faults of the Madison fault system locally have downdropped thrusts of the Hilgard thrust system into the Madison Valley where they are now buried under basin fill; elsewhere the Hilgard thrust system lies as much as 10 km east of the Madison fault zone.

## ACKNOWLEDGMENTS

Special thanks are extended to C.J. Schmidt and his students, whose work in the area permitted my extending the story this far. Insightful reviews by P.G. DeCelles, E.A. Erslev, D.R. Lageson and J.M. O'Neill greatly improved the manuscript.

## REFERENCES

- Baltz, E.H., and O'Neill, J.M., 1984, Geologic map and cross sections of the Mora River area, Sangre de Cristo Mountains, Mora County, New Mexico: U.S. Geological Survey Miscellaneous Investigations Map I-1456, scale 1:24,000.
- Berg, R.B., 1979, Precambrian geology of the west part of the Greenhorn Range, Madison County, Montana: Montana Bureau of Mines and Geology Map 6, scale 1:28,160.
- Berg, R.R., 1962, Mountain flank thrusting in Rocky Mountain foreland, Wyoming and Colorado; American Association of Petroleum Geologists Bulletin, v. 46, p. 2019-2032.
- Chase, R.B., Schmidt, C.J., and Erslev, E.A. (eds.), in press, Laramide basement deformation: Geological Society of America Special Paper.
- DeCelles, P.G., Tolson, R.B., Graham, S.A., Smith, G.A., Ingersoll, R.V., White, J., Schmidt, C.J., Rice, R., Moxon, I., Lemke, L., Handschy, J.W., Follo, M.F., Edwards, D.P., Cavazza, W., Caldwell, M, and Bargar, E., 1987, Laramide thrust-generated alluvial-fan sedimentation, Sphinx Conglomerate, southwestern Montana, American Association of Petroleum Geologists, v. 71, p. 135-155.
- Donath, F.A., and Parker, R.B., 1964, Folds and folding: Geological Society of America Bulletin, v. 75, p. 45-62.
- Erslev, E.A., 1986, Basement balancing of Rocky Mountain foreland uplifts: Geology, v. 14, p. 259-262.
- Erslev, E.A., in press, Thrusts, back-thrusts and detachment of Rocky Mountain foreland arches, *in* Chase, R., Erslev, E.A., and Schmidt, C.J., eds., Basement-cover kinematics of Laramide foreland uplifts: Geological Society of America Special Paper.
- Erslev, E.A., and Rogers, J.L., in press, Basement-cover geometry of Laramide fault-propagation folds, *in* Chase, R., Erslev, E.A., and Schmidt, C.J., eds., Basement-cover kinematics of Laramide foreland uplifts: Geological Society of America Special Paper.
- Fields, R.W., Rasmussen, D.L., Tabrum, A.R., and Nichols, Ralph, 1985, Cenozoic rocks of the intermontane basins of western Montana and eastern Idaho--a summary, *in* Flores, R.M., and Kaplan, S.S., eds., Cenozoic paleogeography of west-central United States: Society of Economic Paleontologists and Mineralogists, Rocky Mountain Section, p. 9-36.
- Garihan J.M., Schmidt, C.J., Young, S.W., and Williams, M.A., 1983, Geology and recurrent movement history of the Bismark-Spanish Peaks-Gardiner fault systems, southwest Montana, *in* Lowell, J.D., and Gries, Robbie, eds., Rocky Mountain Foreland Basins and uplifts: Rocky Mountain Association of Geologists, p. 295-314.
- Hadley, J.D., 1969, Geologic map of Cameron Quadrangle, Madison County, Montana: U.S. Geological Survey Map GQ-813, scale 1:62,500.
- Hanneman, D.L., and Wideman, D.J., 1991, Sequence stratigraphy

- of Cenozoic continental rocks, southwestern Montana: Geological Society of America Bulletin, v. 103, p. 1335-1345.
- Kellogg, K.S., 1990, Laramide cross-crestral thrusting in the northern Madison Range, southwestern Montana [abs.]: Geological Society of America Abstracts with Programs, v. 22, no. 6, p. 16.
- Kellogg, K.S., 1992, Geologic map of the Fan Mountain quadrangle, Madison County, Montana: U.S. Geological Survey Quadrangle Map GQ-1706, scale 1:24,000.
- \_\_\_\_\_, 1993a, Geologic map of the Cherry Lake quadrangle, Madison County, Montana: U.S. Geological Survey Quadrangle Map GQ-1725, scale 1:24,000.
- \_\_\_\_\_, 1993b, Geologic map of the Ennis Lake quadrangle, Madison County, Montana: U.S. Geological Survey Quadrangle Map GQ-17\_\_\_\_, scale 1:24,000.
- Kellogg, K.S., and Harlan, S.S., 1991, Style and timing of deformation in the northwestern Madison Range, southwestern Montana: Geological Society of America Abstracts with Programs, v. 23, no. 4, p. 38.
- Kuenzi, W.D., and Fields, R.W., 1971, Tertiary stratigraphy, structure, and geologic history, Jefferson Basin, Montana: Geological Society of America Bulletin, v. 82, p. 3373-3394.
- Lageson, D.R., 1989, Reactivation of a Proterozoic continental margin, Bridger Range, southwestern Montana, *in* French, D.E., and Grabb, R.F., eds., Geologic resources of Montana, vol. 1: Montana Geological Society, p. 279-298.
- Lageson, D.R., and Zim, J.C., 1985, Uplifted basement wedges in the northern Rocky Mountain foreland: Geological Society of America Abstracts with Programs, v. 7, no. 4, p. 250-251.
- McBride, B.C., Schmidt, C.J., Guthrie, G.E., and Sheedlo, M.K., 1992, Multiple reactivation of a collisional boundary--an example from southwestern Montana, *in* Bartholomew, M.J., Hyndman, D.W., Mogk, D.W., and Mason, R., eds., Basement Tectonics 8--Characterization and comparison of ancient and Mesozoic continental margins: Proceedings of the 8th International Conference of Basement Tectonics, Kluwer Academic Publishers, Dordrecht, The Netherlands, p. 341-357.
- McMannis, W.J., and Chadwick, R.A., 1964, Geology of the Garnet Mountain quadrangle, Gallatin County, Montana: Montana Bureau of Mines and Geology Bulletin 43, 47 p.
- Miller, E.W., and Lageson, D.R., in press, Influence of basement foliation attitude on geometry of Laramide basement deformation, southern Bridger Range and northern Gallatin Range, Montana, *in* Chase, R.B., Schmidt, C.J., and Erslev, E.A., eds., Laramide basement deformation: Geological Society of America Special Paper
- O'Neill, J.M., 1983, Geologic map of the Middle Mountain-Tobacco Root roadless area, Madison County, Montana: U.S. Geological Survey Miscellaneous Field Studies map MF-1590-A, scale 1:50,000.
- O'Neill, J.M., Schmidt, C.J., and Genovese, P.W., 1990, The

- Dillon cutoff--basement involved tectonic link between the disturbed belt of west-central Montana and the overthrust belt of extreme southwestern Montana: *Geology*, v. 18, p. 1107-1110.
- Pardee, J.T., 1950, Late Cenozoic block faulting in western Montana: *Geological Society of America Bulletin*, v. 61, p. 359-406.
- Peale, A.C., 1896, Description of the Three Forks Sheet, Montana: U.S. Geological Survey Geologic Atlas Folio 24, 5 p.
- Perry, W.J., Jr., Haley, J.C., Nichols, D.J., Hammons, P.M., and Ponton, J.D., 1988, Interaction of Rocky Mountain foreland and Cordilleran thrust belt in Lima region, southwest Montana, *in* Schmidt, C.J. and Perry, W.J., Jr., eds., *Interaction of the Rocky Mountain foreland and the Cordilleran thrust belt*: Geological Society of America Memoir 171, p. 267-290.
- Ramsay, J.G., and Huber, M.I., 1987, *The techniques of modern structural geology--volume 2, Folds and fractures*: London, The Academic Press, 462 p.
- Rasmussen, D.L., and Fields, R.W., 1983, Structural and depositional history, Jefferson and Madison basins, southwestern Montana: *American Association of Petroleum Geologists Bulletin*, v. 67, p. 1352.
- Reid, R.R., 1957, Bedrock geology of the north end of the Tobacco Root Mountains, Madison County, Montana: *Montana Bureau of Mines and Geology Memoir* 36, 25 p.
- Ross, C.P., Andrews, D.A., and Witkind, I.J., 1955, Geologic map of Montana: U.S. Geological Survey Map, scale 1:500,000.
- Samuelson, K.J. and Schmidt, C.J., 1981, Structural geology of the western Tobacco Root Mountains, southwestern Montana, *in* Tucker, T.E., ed., *Guidebook of the Montana Geological Society Field Conference and Symposium: Dillon, 1981*, p. 191-199.
- Schmidt, C.J., and Chase, R.B., 1989, Behavior of foliated basement in Rocky Mountain foreland folds, southwestern Montana: *Geological Society of America Abstracts with Programs*, v. 21, no. 5, p. 140.
- Schmidt, C.J., and Dresser, H., 1984, Late Cenozoic structural inversion in a region of small extensional strain, SW Montana: *Geological Society of America Abstracts with Programs*, v. 16, no. 6, p. 646-647.
- Schmidt, C.J., Evans, J.P., Harlan, S.S., Weberg, E.D., Brown, J.S., Batatian, D., Deer, D.N., Malizzi, L., McDowell, R.J., Nelson, G.C., and Parke, M., *in press*, Mechanical behavior of basement rocks during movement of the Scarface thrust, central Madison Range, Montana, *in* Chase, R.B., Schmidt, C.J., and Erslev, E.A., eds., *Laramide basement deformation*: Geological Society of America Special Paper.
- Schmidt, C.J., and Garihan, J.M., 1983, Laramide tectonic development of the Rocky Mountain foreland in southwestern Montana, *in* Lowell, J., ed., *Rocky Mountain foreland basins and uplifts*: Rocky Mountain Association

- of Geologists, p. 271-294.
- \_\_\_\_\_, 1986, Role of recurrent movement of northwest-trending basement faults in the tectonic evolution of southwestern Montana: Proceedings of the 6th International Conference on Basement Tectonics, p. 1-15.
- Schmidt, C.J., Sheedlo, Mark, and Werkema, Michael, 1984, Control of range-bounding normal faults by earlier structures, southwestern Montana [abs.]: Geological Society of America Abstracts with Programs, v. 16, no. 4, p. 253.
- Scholten, Robert, 1967, Structural framework and oil potential of extreme southwestern Montana: Montana Geological Society 18th Annual Field Conference Guidebook, p. 7-19.
- Sharry, J., Langen, R.T., Jovanovich, D.B., Jones, G.M., Hill, N.R., and Guidish, T.M., 1986, Enhanced imaging of the COCORP seismic line, Wind River Mountains, in Barazangi, M., and Brown, L., eds., Reflection seismology--a global perspective: American Geophysical Union Geodynamics Series, v. 13, p. 223-236.
- Sheedlo, M.K., 1984, Structural geology of the northern Snowcrest Range, Beaverhead and Madison Counties, Montana: Kalamazoo, Western Michigan University, M.S. Thesis, 132 p.
- Smith, R.B., and Sbar, M.L., 1974, Contemporary tectonics and seismicity of the western United States, with emphasis on the intermountain seismic belt: Geological Society of America Bulletin, v. 85, p. 1205-1218.
- Spang, J.H., Evans, J.P., and Berg, R.R., 1985, Balanced cross sections of small fold-thrust structures: The Mountain Geologist, v. 22, p. 41-46.
- Swanson, R.W., 1950, Geology of part of the Virginia City and Eldridge quadrangles, Montana: U.S. Geological Survey Open-File Report 51-4, 12 p.
- Tonnson, J.J., 1982, Zone of impingement between the western thrust belt and the foreland province in the Madison and Gallatin Ranges, southwestern Montana, in Powers, W., ed., The western overthrust belt from Alaska to Mexico: Rocky Mountain Association of Geologists, p. 185-192.
- Tysdal, R.G., 1976, Geologic map of the northern part of the Ruby Range, Madison County, Montana: U.S. Geological Survey Miscellaneous Investigations Series Map I-951, scale 1:24,000.
- \_\_\_\_\_, 1986, Thrust faults and back thrusts in Madison Range of southwest Montana foreland: American Association of Petroleum Geologists Bulletin, v. 70, p. 360-376.
- \_\_\_\_\_, 1990, Geologic map of the Sphinx Mountain quadrangle and adjacent parts of the Cameron, Cliff Lake, and Hebgen Dam quadrangles, Montana: U.S. Geological Survey Miscellaneous Investigations Series Map I-1815, scale 1:62,500.
- Tysdal, R.G., Marvin, R.F., and DeWitt, E.H., 1986, Late Cretaceous stratigraphy, deformation, and intrusion in the Madison Range of southwestern Montana: Geological Society of America Bulletin, v. 97, p. 859-868.
- Tysdal, R.G., and Simons, F.S., 1985, Geologic map of the Madison

- Roadless area, Gallatin and Madison Counties, Montana: U.S. Geological Survey Miscellaneous Field Studies Map MF-1605-B, scale 1:96,000.
- U.S. Geological Survey, 1964, The Hebgen Lake, Montana, earthquake of August 17, 1959: U.S. Geological Survey Professional Paper 435, p. 37-50.
- Werkema, M.A., and Young, S.W., 1983, Overlapping styles of deformation, northern Madison Range, Montana: Geological Society of America Bulletin Abstracts with Programs, v. 15, no. 5, p. 296.
- Wooden, J.L., Vitaliano, C.J., Koehler, S.W., and Ragland, P.C., 1978, The late Precambrian mafic dikes of the southern Tobacco Root Mountains, Montana--geochemistry, Rb-Sr geochronology, and relationship to Belt tectonics: Canadian Journal of Earth Sciences, v. 15, p. 467-479.
- Young, S.W., 1985, Structural history of the Jordan Creek area, northern Madison Range, Madison County, Montana: Austin, Texas, University of Texas, M.A. thesis, 113 p.

## FIGURES

Figure 1. Simplified geologic map of the southwestern Montana foreland province. Cross-section A-A' is shown in Figure 10B. Numbered localities refer to (1) Hilgard thrust system of Tysdal (1986) and (2) normal faults of the Madison Range fault system of Pardee (1950). Modified from Schmidt and Garihan (1986), Tysdal, (1986), Sheedlo (1984), Ross and others (1955), Perry and others (1988), and O'Neill and others (1990).

Figure 2. Geologic map of the study area in the northwestern Madison Range, simplified from Kellogg (1992, 1993a). Numbered locations are discussed in text. Trend lines shown within basement rocks reflect foliation attitudes actually mapped.

Figure 3. Interpretive cross sections, the traces of which are shown on Figure 2. More detail is given in Kellogg (1992, 1993a).

- A. Cross section A-A'.
- B. Cross section B-B'.
- C. Cross section C-C', approximately along Jack Creek.
- D. Cross section D-D'.
- E. Cross section E-E', through Shell Creek.

Figure 4. Photograph looking northwest across Jack Creek toward the intersection of the Hilgard thrust system and the Spanish Peaks fault. Symbols are same as in Figure 2 with these additions: Kd (dacite porphyry sill), Kmo (Mowry Shale), Kmd (Muddy Sandstone), Kt (Thermopolis shale), Kk (Kootenai Formation), Ps (Shedhorn Sandstone), and Pq (Quadrant Sandstone).

Figure 5. Graph showing increasing net dip separation of basement-cover contact along faults of the Hilgard thrust system vs. distance south from the Spanish Peaks fault. See Figure 2 for locations of cross sections.

Figure 6. Photograph looking north toward Shell Creek canyon. Symbols are same as in Figure 2 with these additions: Kd (dacite porphyry sill), Kmo (Mowry Shale), Kmd (Muddy Sandstone), Kt (Thermopolis shale), Kk (Kootenai Formation), Ps (Shedhorn Sandstone), and Pq (Quadrant Sandstone).

Figure 7. Cross section E-E' (Fig. 6E) restored to area-balanced, post-Laramide, pre-extensional configuration.

Figure 8. Equal-area (Schmidt), lower-hemisphere projection of contoured poles to foliation in Archean rocks within area 5a (defined by dashed line in Fig. 2) directly north of the Spanish Peaks fault (31 observations) and fault block 5b (Fig. 2), immediately south of Spanish Peaks fault and west of Hilgard thrust system (33 observations; includes some data of Young, 1985). Computer-determined contour intervals are 5, 10, and 15 percent per one percent area.

Figure 9. Schematic model for Laramide basement rotation at inception (A) and close (B) of Laramide deformation.

Figure 10. East-west cross sections across a portion of southwestern Montana showing major tectonic elements for: (A) the close of Laramide deformation, and (B) the present. The location of cross-section A-A' (Fig. 10B) and unit symbols are given Figure 1. Adapted, in part, from Schmidt and others (1984), Sheedlo (1984), Sharry and others, (1986), and McBride and others, (1992).



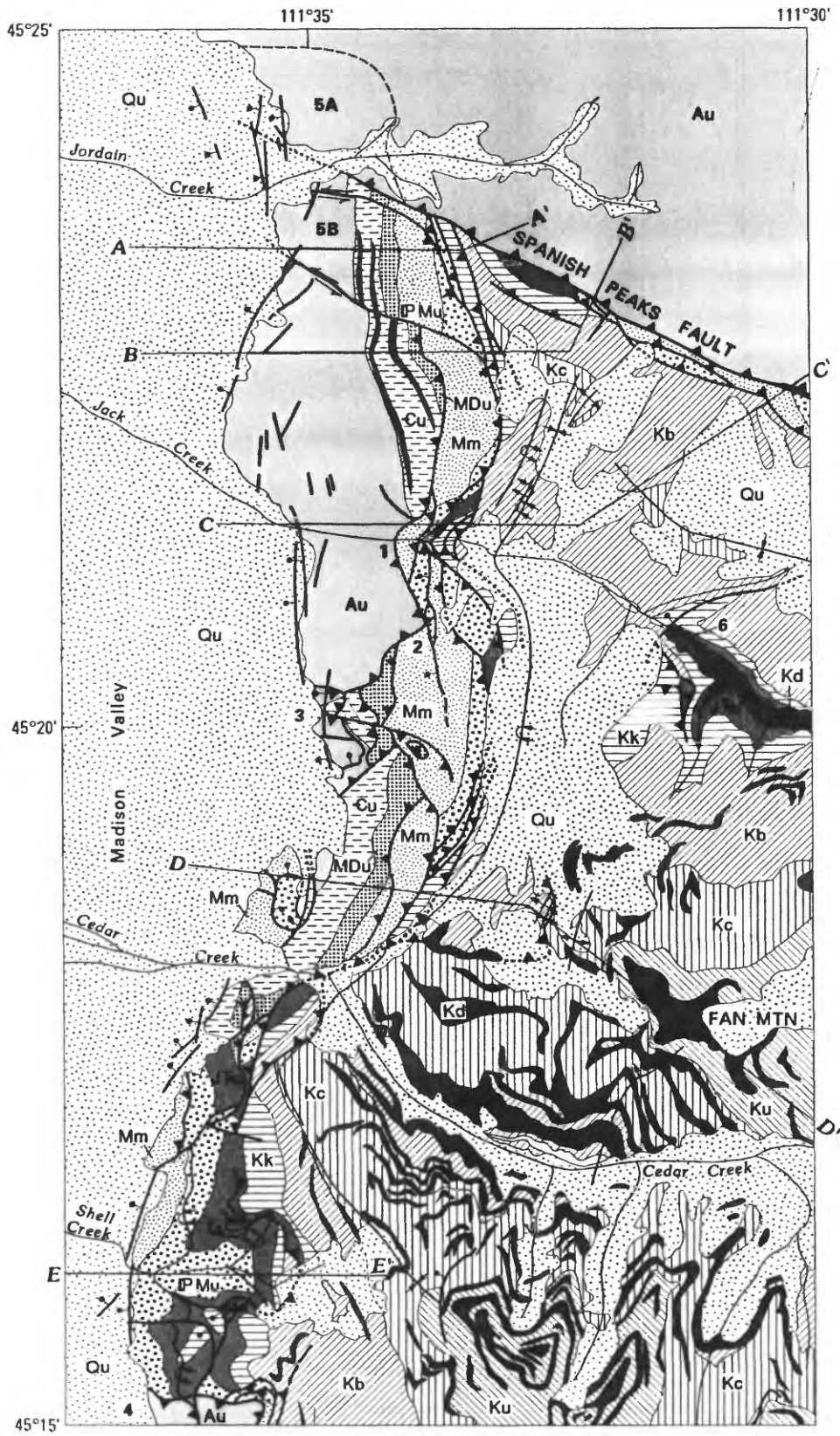


Fig. 2

**EXPLANATION**

- 
**QTu** Quaternary, undifferentiated
- 
**Kd** Fan Mountain Dacite
- 
**Ku** Everts (?) Formation, Virgelle Sandstone and Telegraph Creek Formation
- 
**Kc** Cody Shale
- 
**Kb** Frontier Formation, Mowry Shale, Muddy Sandstone, and Thermopolls Shale
- 
**Kk** Kootenal Formation
- 
**M** Morrison Formation, Eells Group, and Dinwoody Formation
- 
**PMu** Shedhorn and Quadrant Sandstones, and Amsden and Snowcrest Range Groups
- 
**Mm** Madison Group: Mission Canyon and Lodgepole Limestones
- 
**MDu** Three Forks and Jefferson Formations
- 
**Cu** Cambrian, undifferentiated
- 
**Au** Archean, undifferentiated

 **Thrust or reverse fault**—Dashed where inferred; dotted where concealed; teeth on upper plate

 **Normal fault**—Dashed where inferred; dotted where concealed; bar and ball on downthrown side

 **Anticline**

 **Overturned anticline**

 **Syncline**

 **Overturned syncline**



Fig. 2 (con'd)

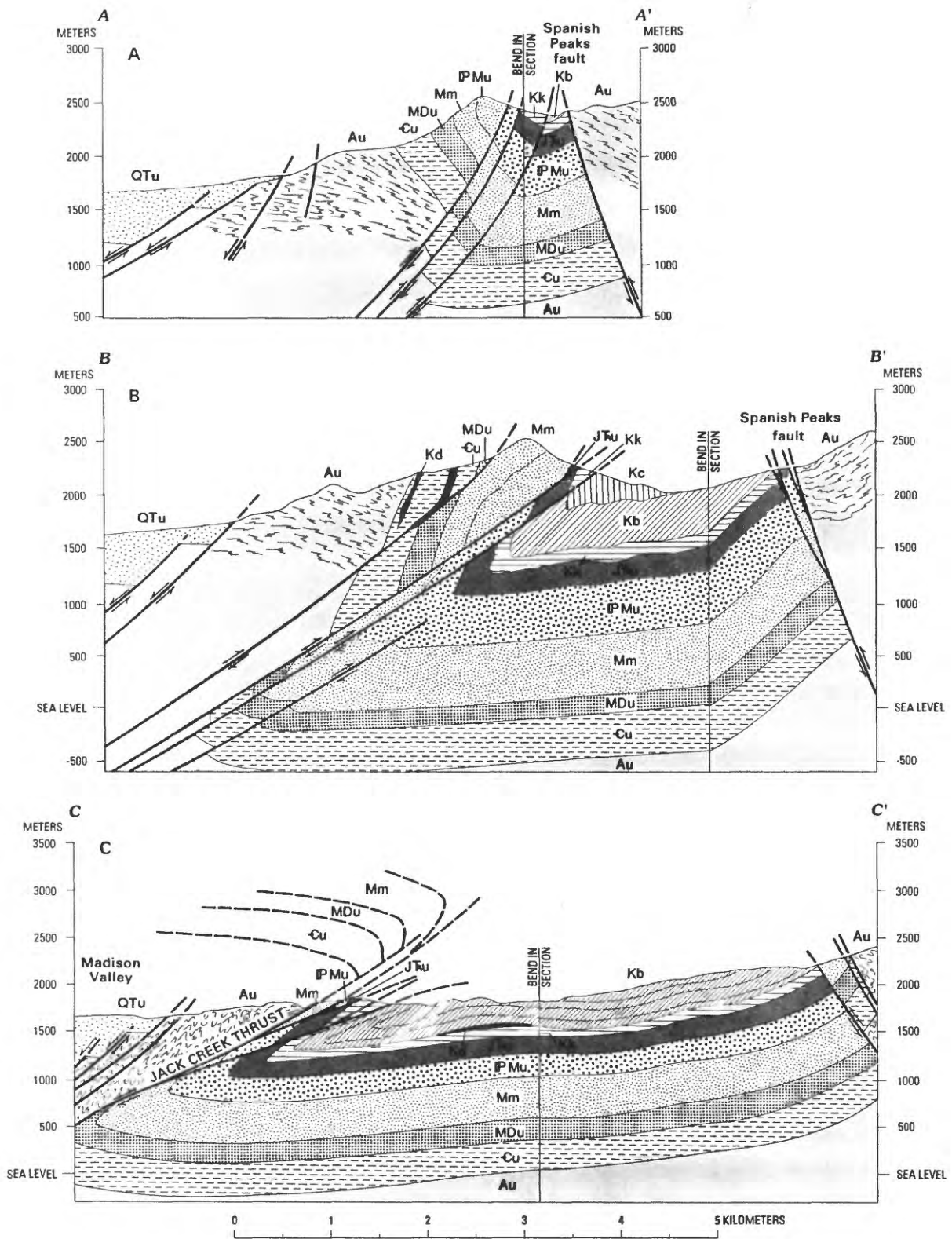


Fig.3

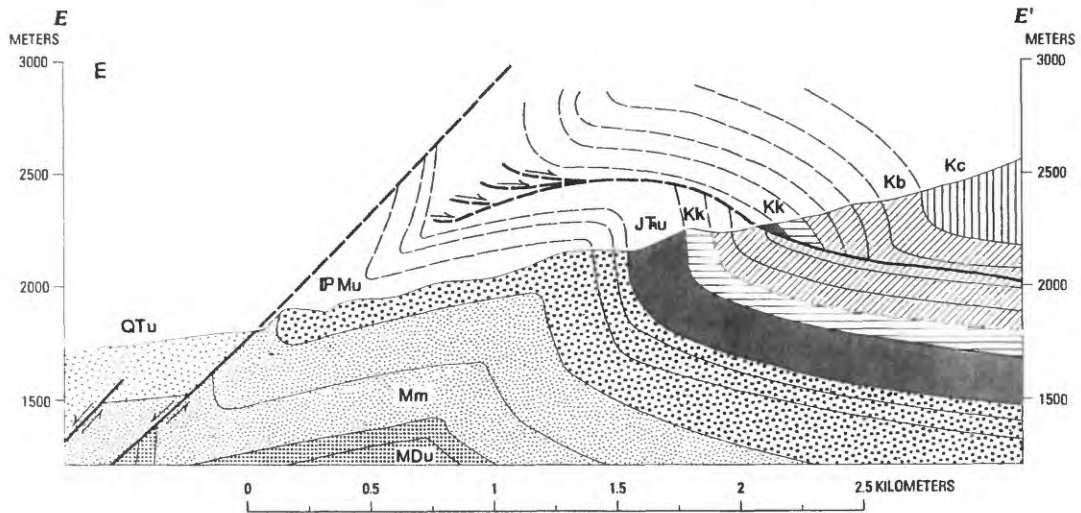
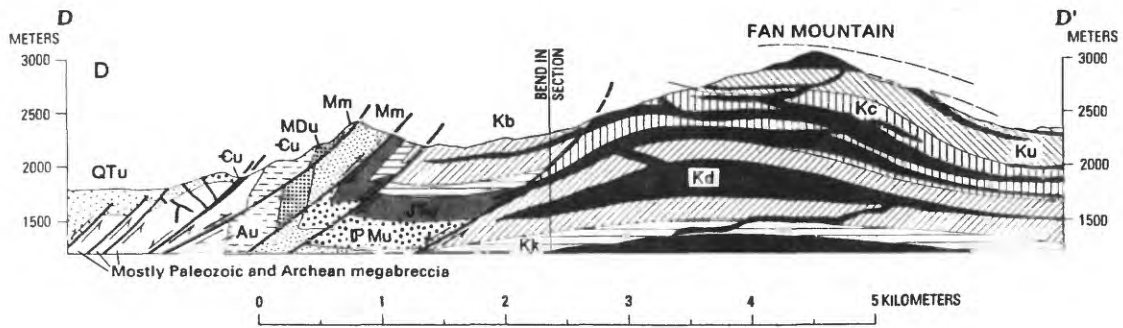
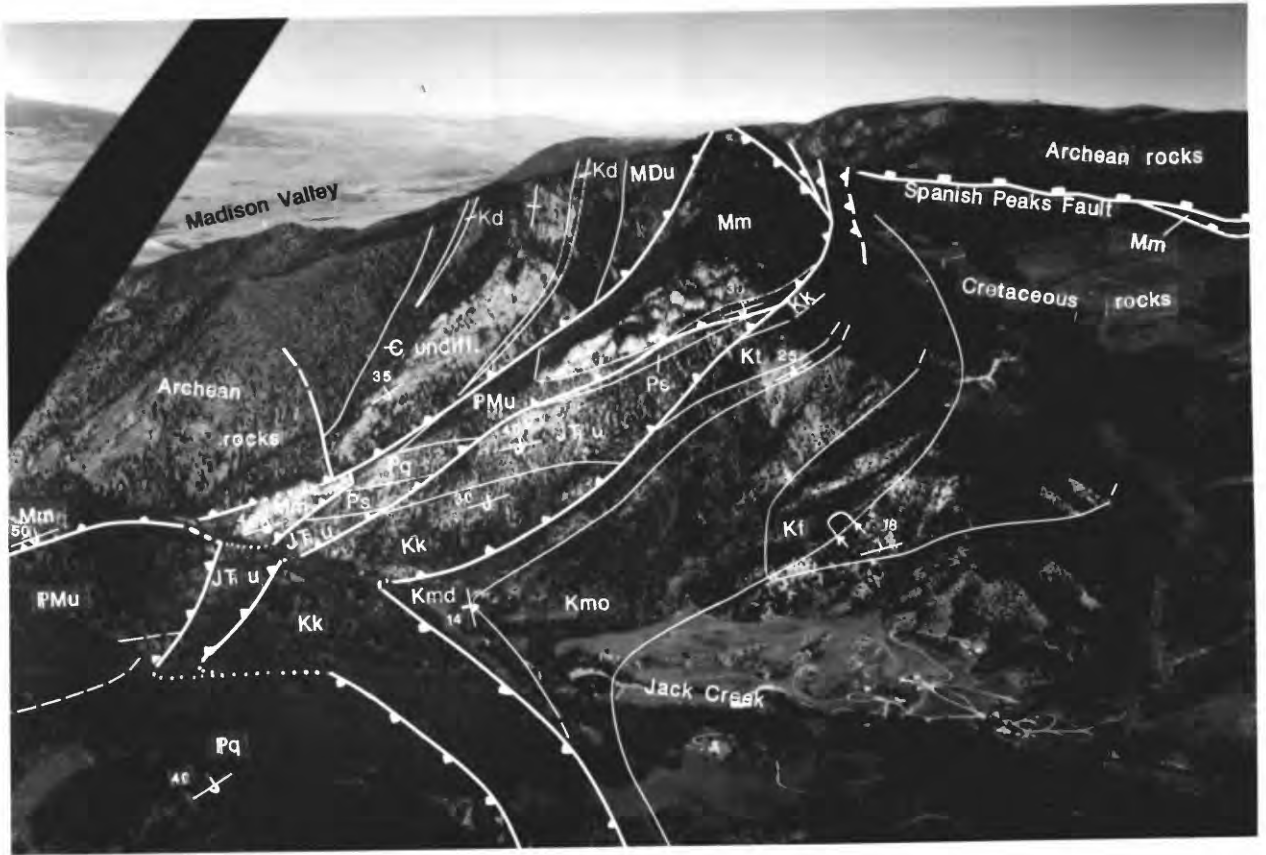


Fig. 3 (cont'd)



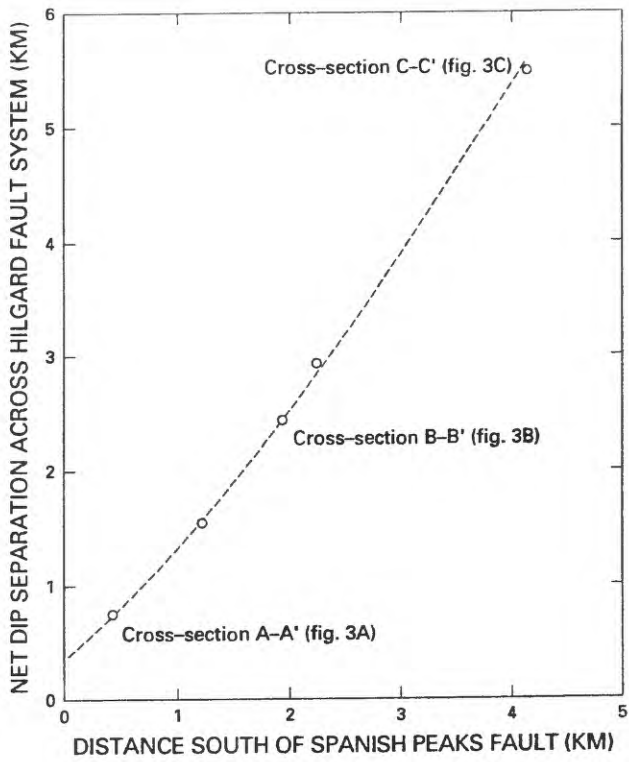


Fig. 5



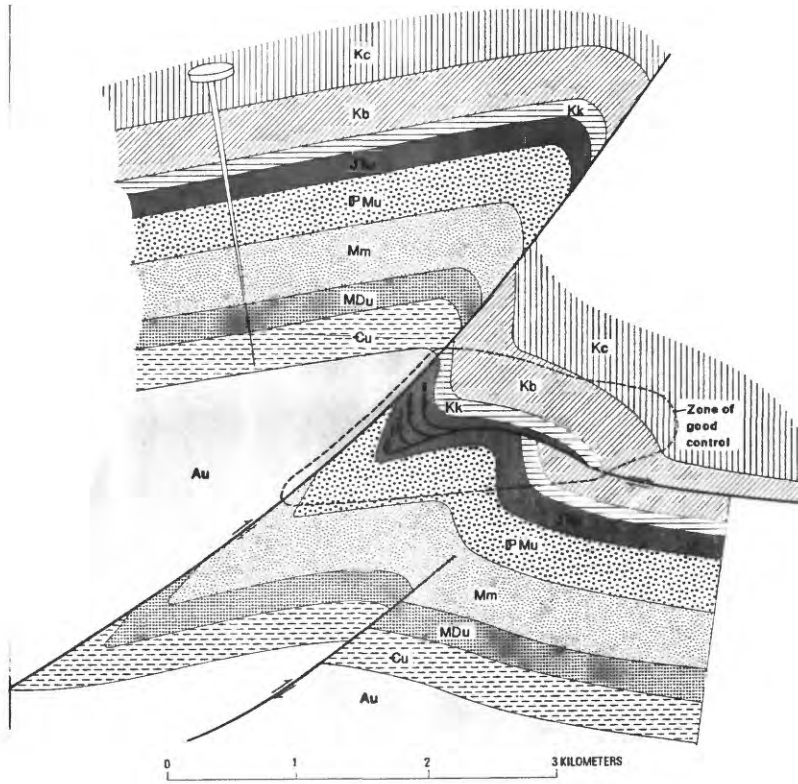


Fig. 7

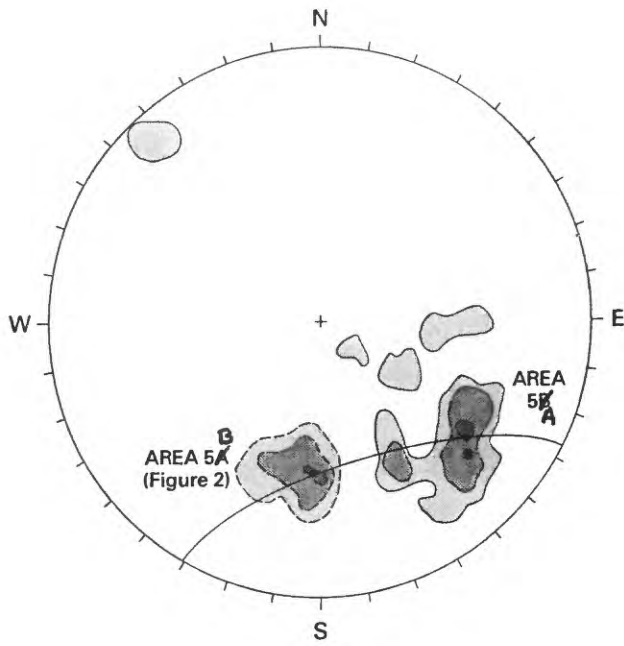


Fig. 8

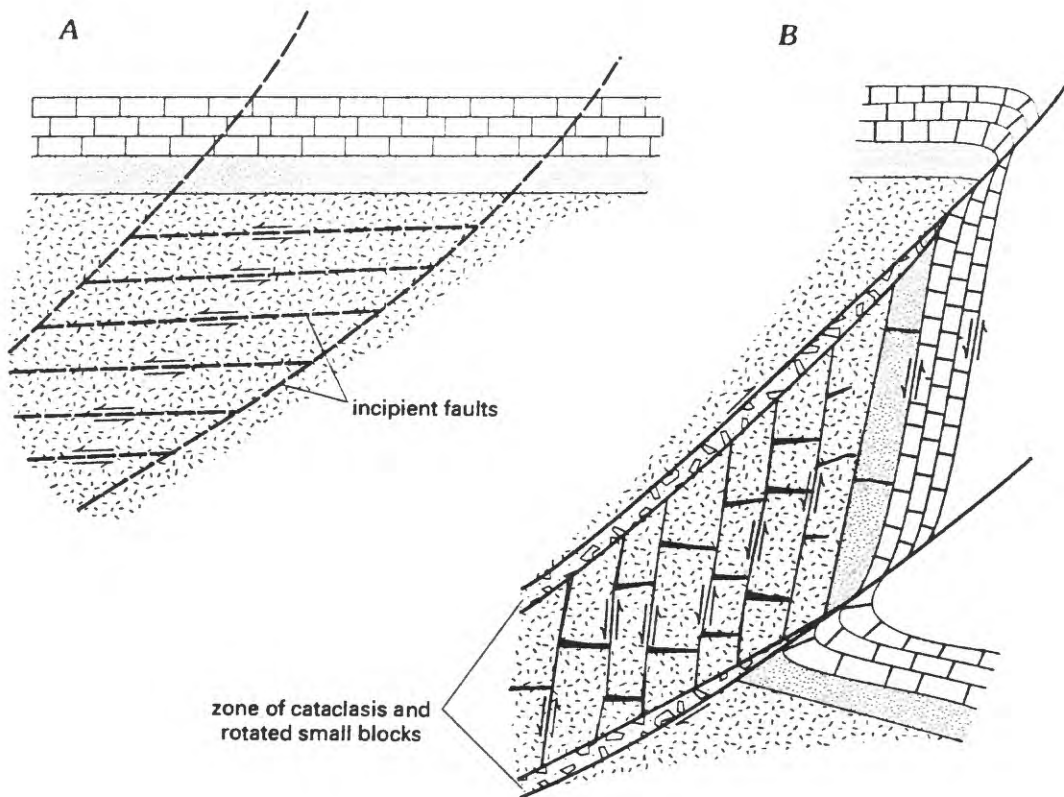


Fig. 9

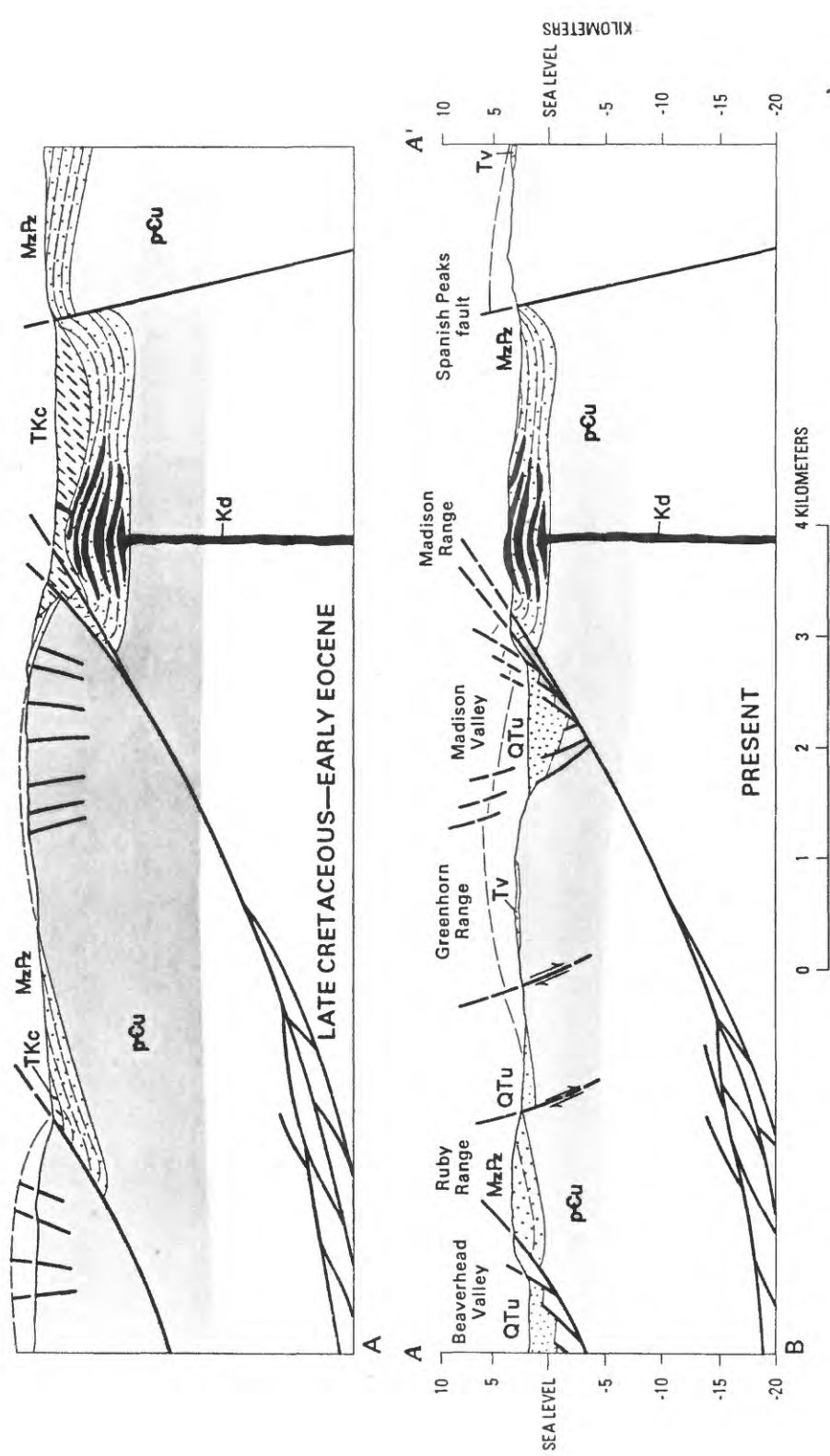


Fig. 10